Development 127, 2347-2355 (2000)
Printed in Great Britain © The Company of Biologists Limited 2000
DEV4283

The *Oak Ridge Polycystic Kidney* (*orpk*) disease gene is required for left-right axis determination

Noel S. Murcia[1,*], William G. Richards[2,*], Bradley K. Yoder[3,*], Michael L. Mucenski[4], John R. Dunlap[5] and Richard P. Woychik[1,6,‡]

[1]Department of Pediatrics, Rainbow Babies and Children's Hospital, Case Western Reserve University, Cleveland, OH 44106, USA
[2]Neuroscience Department, Amgen, Thousand Oaks, CA 91320, USA
[3]Department of Cell Biology, University of Alabama at Birmingham, Birmingham, AL 35294, USA
[4]Division of Pulmonary Biology, Children's Hospital Medical Center, Cincinnati, OH 45229, USA
[5]The Program in Microscopy, The University of Tennessee, Knoxville, TN 37996, USA
[6]Parke-Davis Laboratory for Molecular Genetics, Alameda, CA 94502, USA
*These authors contributed equally to this manuscript
‡Author for correspondence at address 6 (e-mail: Rick.Woychik@wl.com)

Accepted 6 March; published on WWW 10 May 2000

SUMMARY

Analysis of several mutations in the mouse is providing useful insights into the nature of the genes required for the establishment of the left-right axis during early development. Here we describe a new targeted allele of the mouse *Tg737* gene, *Tg737*$^{\Delta 2\text{-}3\beta Gal}$, which causes defects in left-right asymmetry and other abnormalities during embryogenesis. The *Tg737* gene was originally identified based on its association with the mouse *Oak Ridge Polycystic Kidney* (*orpk*) insertional mutation, which causes polycystic kidney disease and other defects. Complementation tests between the original *orpk* mutation and the new targeted knock-out mutation demonstrate that *Tg737*$^{\Delta 2\text{-}3\beta Gal}$ behaves as an allele of *Tg737*. The differences in the phenotype between the two mutations suggest that the *orpk* mutation is a hypomorphic allele of the *Tg737* gene. Unlike the *orpk* allele, where all homozygotes survive to birth, embryos homozygous for the *Tg737*$^{\Delta 2\text{-}3\beta Gal}$ mutation arrest in development at mid-gestation and exhibit neural tube defects, enlargement of the pericardial sac and, most notably, left-right asymmetry defects. At mid-gestation the direction of heart looping is randomized, and at earlier stages in development *lefty-2* and *nodal*, which are normally expressed asymmetrically, exhibit symmetrical expression in the mutant embryos. Additionally, we determined that the ventral node cells in mutant embryos fail to express the central cilium, which is a characteristic and potentially functional feature of these cells. The expression of both *Shh* and *Hnf3β* is downregulated in the midline at E8.0, indicating that there are significant alterations in midline development in the *Tg737*$^{\Delta 2\text{-}3\beta Gal}$ homozygous embryos. We propose that the failure of ventral node cells to fully mature alters their ability to undergo differentiation as they migrate out of the node to contribute to the developing midline structures. Analysis of this new knockout allele allows us to define a critical role for the *Tg737* gene during early embryogenesis. We have named the product of the *Tg737* gene Polaris, which is based on the various polarity related defects associated with the different alleles of the *Tg737* gene.

Key words: Situs inversus, Neural tube defect, Left-right asymmetry, Ventral node cilia, Targeted mutation, Insertional mutation, Complementation, Tg737, ORPK, Polaris

INTRODUCTION

Asymmetric positioning of visceral organs is determined by the left-right axis. Left-right determination is most critical to cardiovascular development, where precise alignment along the left-right axis is required for proper circulation and viability. Development fails if the heart does not loop from its initial midline orientation. Complete reversal of organ position, designated situs inversus, is compatible with normal development and viability. However, defects in consistently positioning organs along the left-right axis (situs ambiguous) are more clinically relevant and can lead to polysplenia, asplenia, cardiac and/or circulatory defects (Casey, 1998).

The mechanism that generates adult left-right asymmetry from a bilaterally symmetric embryo may involve a stepwise process of (1) generation of an initial asymmetric signal; (2) propagation and spatial maintenance of asymmetric information; and (3) transformation of these signals into morphological asymmetries. Based on the presence of a left-right phenotype and/or left-right asymmetrical expression, several genes have been identified that either act at early, middle or late steps in this pathway. *Inversin* and *left-right*

dynein appear to be involved in early steps of the left-right determination (Supp et al., 1997; Mochizuki et al., 1998; Morgan et al., 1998). Clues as to how a signal may be asymmetrically localized have emerged with the analysis of *KIF3B* mutants, and the finding that cilia on ventral node cells appear to generate an asymmetric flow across the node surface of primitive streak-stage embryos (Nonaka et al., 1998). This flow may create an asymmetric distribution of signaling molecules, establishing a left-right gradient across the node. Propagation and maintenance of initial asymmetry may be mediated through the actions of *lefty-1* at the midline, and *lefty-2* and *nodal* in lateral plate mesoderm (Meno et al., 1998). Interpretation of molecular asymmetries into physical asymmetries may involve transcription factors such as *Pitx2* (Ryan et al., 1998).

Many aspects relating to the establishment of left-right asymmetry during development are unknown. It would be useful to have a better understanding of the nature of the molecular signals that initiate this process. Access to additional mouse mutants that exhibit an early stage phenotype in the establishment of the left-right axis would be useful in this regard. Here we describe a new mutation, which appears to affect the early stages of left-right specification during embryogenesis. Utilizing targeted mutagenesis, we created a new allele of an existing gene, *Tg737*, which was originally identified by its association with the *Oak Ridge Polycystic Kidney* (*orpk*) mouse model of autosomal recessive polycystic kidney disease (ARPKD) (Moyer et al., 1994). Analysis of the phenotype associated with this new allele places the *orpk* gene early in the pathway of left-right determination.

MATERIALS AND METHODS

Generation of the *Tg737$^{\Delta 2\text{-}3\beta Gal}$* allele

The *Tg737$^{\Delta 2\text{-}3\beta Gal}$* allele of the *Tg737* gene was generated by homologous recombination in embryonic stem cells. Briefly, 1×10^7 ESCS cells (a gift from Dr Colin Stewart) were electroporated with 25 μg of *Not*I linearized targeting plasmid in a BioRad gene pulsar (320 V, 500 μF) and placed under G418 selection as previously described (Hogan et al., 1994). Genomic DNA from G418 resistant colonies was screened for recombinants by Southern blotting analysis as described below. Seven out of 196 clones were found to contain a targeted mutation in the *Tg737* gene (Fig. 1B). Targeted clones were injected into C57BL/6J blastocysts. Chimeric males were bred to FVB/N females to establish germline transmission of the *Tg737$^{\Delta 2\text{-}3\beta Gal}$* allele.

Construction of the targeting vector

The targeting construct used for the homologous recombination experiments was produced utilizing the pSAβ-Gal plasmid (a gift from Dr P. Soriano). A genomic clone containing the 5′ region of the *Tg737* gene was isolated from a 129/Sv genomic lambda library using probes corresponding to exons 1 and 2 of the *Tg737* gene. A 6.4 kb *Not*I/*Cla*I genomic fragment containing exon 1 was subcloned between the *Not*I and *Sma*I sites (after blunt-ending the *Cla*I overhang) upstream of the SA*β-Gal/pgk-neo* cassette. Additionally, a 2.1 kb PCR fragment containing intron 3 and part of the flanking exons was amplified using standard PCR conditions from 129/Sv genomic DNA using primers that introduced *Sal*I sites into the ends of the amplified product (primers: RW416 5′-tga ggt cga cac ggg ttt tca gca agc a-3′ forward and RW415 5′-ctc tgt cga ctg ctg tgc ttg gta t-3′ reverse). After digestion with *Sal*I, this 2.1 kb PCR-derived fragment was cloned into the *Sal*I site downstream of the SA*β-Gal/pgk-neo* cassette. All cloning steps followed standard methodology (Sambrook et al., 1989).

Genotyping animals and embryos

A 1 kb intron 4-specific probe, which is outside the targeting construct, was utilized to identify the targeted allele at the molecular level. This intron 4 probe was generated by standard PCR amplification from genomic DNA (primers: RW436 5′-gca gac cca tag cta ctg ga-3′ forward and RW239 5′-ctt ccc att gat gat gtc ag-3′ reverse). In genomic DNA samples digested with *Bam*HI, the intron 4 probe hybridizes to a 7 kb band from the mutant allele and to a 20 kb fragment on the wild-type allele (Fig. 1B). The *orpk* insertional mutation was identified as previously described and is depicted in Fig. 1A (Moyer et al., 1994).

Embryos from *Tg737$^{\Delta 2\text{-}3\beta Gal}$* heterozygous parents were routinely analyzed by PCR using standard conditions and primers specific for the targeted mutant allele (primers: RW472 5′-agc aga agc ctg cga tgt c-3′ forward and RW473 5′-gtc aga cga ttc att ggc ac-3′ reverse) and primers specific for the wild-type allele (primers: RW597 5′-agt gat atc cgg tac aaa tga tgg aaa atg ttc a-3′ forward and RW598 5′-gag tga ttt cct cag tat cat agg ctg ggt tgt a-3′ reverse). These reactions amplify a targeted specific product of 270 bp and a wild-type product of 170 bp.

RT-PCR analysis

Embryonic day (E)9.5 embryos were isolated from *Tg737$^{\Delta 2\text{-}\beta Gal}$* heterozygous intercrosses and genotyped to identify wild-type, heterozygous and homozygous mutants, as described above. Embryos of the same genotype were pooled and processed for total RNA isolation using RNA STAT-60 (TEL-TEST 'B', INC.). cDNA was synthesized following standard protocols (Sambrook et al., 1989). cDNAs were amplified using standard PCR conditions and primers that amplify from exon 1 to exon 11 (primers: RW117 5′-gga tca ggc gtc gct tct tc-3′ forward and RW92 5′-atc taa ggc cat tcg gta ga-3′ reverse, producing a 851 bp product), exon 2 (RW597, 5′-agt gat atc cgg tac aaa tga tgg aaa atg ttc a-3′, and RW598, 5′-gag tga ttt cct cag tat cat agg ctg ggt tgt a-3′, producing a 170 bp product), and exon 23 to exon 26 of the *Tg737* cDNA (primers: RW71 5′-cgt ctc tgc aca gat att gg-3′ forward and RW118 5′-aca gca caa acc cat cct ca-3′ reverse, producing a 832 bp product). β-Actin mRNA was amplified as a positive control (primers: RW51 5′-atg ggt cag aag gac tcc ta-3′ forward and RW53 5′-ggt gta aaa cgc agc tca gt-3′ reverse, producing a 1020 bp product).

Complementation experiments

Compound heterozygotes were generated by crossing mice heterozygous for the *Tg737$^{\Delta 2\text{-}3\beta Gal}$* allele on the mixed FVBN-129/Sv genetic background with *orpk* heterozygotes on a uniform FVB/N genetic background. Individual animals in the offspring from these crosses were genotyped as described above. As a control for genetic background in evaluating the phenotype, FVB/N *orpk* heterozygotes were crossed with wild-type 129/Sv partners and the resulting F_1 heterozygotes were crossed to FVB/N *orpk* heterozygotes to obtain *orpk* homozygotes in a mixed FVBN-129/Sv genetic background.

Histological and skeletal analysis

For histological examination, tissues were fixed in 10% buffered formalin, embedded in paraffin and cut into 8 μm sections following standard procedures. Tissue sections were stained with Hematoxylin and Eosin, examined and photographed under light microscopy. Skeletal analyses were performed as previously described (Hogan et al., 1994).

Scanning electron microscopy (SEM)

Embryos for SEM analysis were prepared as previously described by Sulik et al. (1994), with slight modifications. Samples were fixed in 2.5% glutaraldehyde, 0.1 M cacodylate buffer overnight, washed twice

in 0.1 M cacodylate, dehydrated through an ethanol series and washed twice in 100% ethanol. Embryos were dried from liquid CO_2, mounted, sputter-coated and viewed using a JEOL scanning electron microscope.

β-Gal reporter gene analysis and mRNA in situ hybridization

Primitive streak-stage (E7.5) and early headfold-stage (E8.0) embryos were collected from timed matings of *Tg737*$^{\Delta 2\text{-}3\beta Gal}$ heterozygous intercrosses and were genotyped as described above. For *β-Gal* reporter analysis, embryos were processed as previously described (Hogan et al., 1994). Whole-mount mRNA in situ hybridizations with anti-sense digoxigenin-labelled riboprobes were performed as previously described (Henrique et al., 1995). Sections of whole-mount stained embryos were obtained as previously described (Hogan et al., 1994). *Lefty-2*, *nodal*, *Shh*, *Hnf3β* and *Brachyury* probes were kindly provided by Drs H. Hamada, M. Kuehn, T. Magnuson and R. Conlon.

RESULTS

Production of the targeted allele, *Tg737*$^{\Delta 2\text{-}3\beta Gal}$

The *Tg737* gene is directly associated with the recessive insertional mutation in the mouse called *orpk*. This mutation causes polycystic kidney disease and other disorders (Moyer et al., 1994). Northern blot analysis demonstrated that the *orpk* mutation alters, but does not completely abolish, all mRNA expression from the *Tg737* gene (Moyer et al., 1994; Yoder et al., 1995). This finding suggested that the *orpk* insertional mutation created a unique allele that does not necessarily completely inactivate the function of the *Tg737* gene. Therefore, to further investigate the function of *Tg737*, we generated a knock-out allele (*Tg737*$^{\Delta 2\text{-}3\beta Gal}$) by homologous recombination in embryonic stem (ES) cells. This new allele was engineered to delete the initial coding exons (exon 2 and part of exon 3) of *Tg737*. This deleted region of *Tg737* was replaced with the *β-Galactosidase* (*β-Gal*) reporter gene (Fig. 1A). We reasoned that this structural configuration would both inactive the expression of the gene and simultaneously allow the *β-Gal* reporter gene to be expressed in place of the normal *Tg737* mRNA.

Seven correctly targeted clones were identified from the 196 clones analyzed, indicating that the targeting efficiency was 3.6% (Fig. 1B). Chimeric males were derived from C57BL/6 blastocysts injected with targeted 129/Sv ES cells, and germline transmission of the *Tg737*$^{\Delta 2\text{-}3\beta Gal}$ allele was obtained by breeding the chimeras to wild-type FVB/N mice. The FVB/N strain was chosen since the *orpk* insertional mutation was generated on this strain. Unless otherwise indicated, most analyses were conducted after six generations inbred into the FVB/N background.

Expression of *Tg737* mRNA transcripts derived from the *Tg737*$^{\Delta 2\text{-}3\beta Gal}$ allele was tested by RT-PCR with total RNA isolated from embryonic day 9.5 (E9.5) wild-type, heterozygous and homozygous *Tg737*$^{\Delta 2\text{-}3\beta Gal}$ embryos. Three different regions of the *Tg737* gene were evaluated for expression using primers that amplify exons 1-11, exon 2 and exons 23-24. *Tg737* transcripts were detected in RNA isolated from wild-type and heterozygous embryos; however, no amplification products were obtained with RNA from homozygous mutants (Fig. 1C). These experiments demonstrate that the *Tg737*$^{\Delta 2\text{-}3\beta Gal}$ allele completely eliminates expression of the Tg737 gene.

Targeted mutation *Tg737*$^{\Delta 2\text{-}3\beta Gal}$ and the *orpk* insertional mutation are allelic

As a first step in characterizing the new *Tg737*$^{\Delta 2\text{-}3\beta Gal}$ allele, we conducted a series of complementation experiments with the original *orpk* insertional mutation. This was an important experiment because the original *orpk* insertional allele arose by random insertion of a transgene and many of these mutants contain structural rearrangements that affect more than one gene. Mice heterozygous for the *Tg737*$^{\Delta 2\text{-}3\beta Gal}$ targeted allele and the *orpk* insertional mutation were crossed to generate offspring that were heterozygous for the *Tg737*$^{\Delta 2\text{-}3\beta Gal}$ or *orpk*, or both, mutations (*Δ2-3βGal/orpk*). Littermates that were heterozygous for either allele had a normal phenotype. However, the compound heterozygotes developed cystic lesions in their kidneys, along with the liver and pancreatic lesions that are typical of the *orpk* mutation on a mixed genetic background (Fig. 2A-I). Additionally, analysis of the skeleton of the compound heterozygotes revealed preaxial polydactyly on all four limbs, which is also a feature of *orpk* homozygotes (Fig. 2J-K) (Moyer et al., 1994). Therefore, our new targeted mutation genetically functions as a second allele of the *Tg737* gene.

Tg737$^{\Delta 2\text{-}3\beta Gal}$ homozygotes undergo developmental arrest

As a follow-up to our complementation experiments, we intercrossed *Tg737*$^{\Delta 2\text{-}3\beta Gal}$ heterozygotes in order to produce individual animals that were homozygous for the *Tg737*$^{\Delta 2\text{-}3\beta Gal}$ mutation. Unlike the *orpk* allele of *Tg737*, where homozygotes could be detected in Mendelian ratios at birth (Moyer et al., 1994), we were unable to detect any *Tg737*$^{\Delta 2\text{-}3\beta Gal}$ homozygotes that survived to birth. This result indicated that homozygosity of the *Tg737*$^{\Delta 2\text{-}3\beta Gal}$ allele causes prenatal lethality. To begin characterizing the lethality we systematically genotyped embryos from heterozygous *Tg737*$^{\Delta 2\text{-}3\beta Gal}$ matings at different stages of development. Between E18.5 and E12.5 no homozygous mutants were obtained (45/139 +/+ and 94/139 Δ2-3βGal/+); at E11.5 homozygotes were obtained, but these embryos exhibited neural tube defects (NTDs) and were not viable (16/56 +/+, 29/56 Δ2-3βGal/+, 11/56 Δ2-3βGal/Δ2-3βGal). Viable homozygous mutants were obtained at normal Mendelian ratios up to E10.5 (29/109 +/+, 56/109 Δ2-3βGal/+, 24/109 Δ2-3βGal/Δ2-3βGal). Analysis of *Tg737*$^{\Delta 2\text{-}3\beta Gal}$ homozygotes at E9.5 revealed that they were runted and exhibited NTDs, including poor differentiation of the forebrain, midbrain, hindbrain, branchial arches, neural tube kinks and undulations of the neural tube (Fig. 3A). At midgestation (E9.5 and E10.5) these embryos exhibited an enlargement of the pericardial sac, indicating that cardiac insufficiency is the most likely cause of lethality in these mutants (Fig. 3A). These embryos also possessed broadened limb buds, a trait that is also characteristic of the embryonic phenotype of *orpk* homozygous mutants (data not shown). All of the embryos used for these experiments were derived from parents that were ten generations inbred in the FVB/N background.

Tg737 is expressed during early post-implantation development in the murine node

In an attempt to identify the earlier stage defects that are likely to give rise to the abnormalities apparent in the mid-gestation

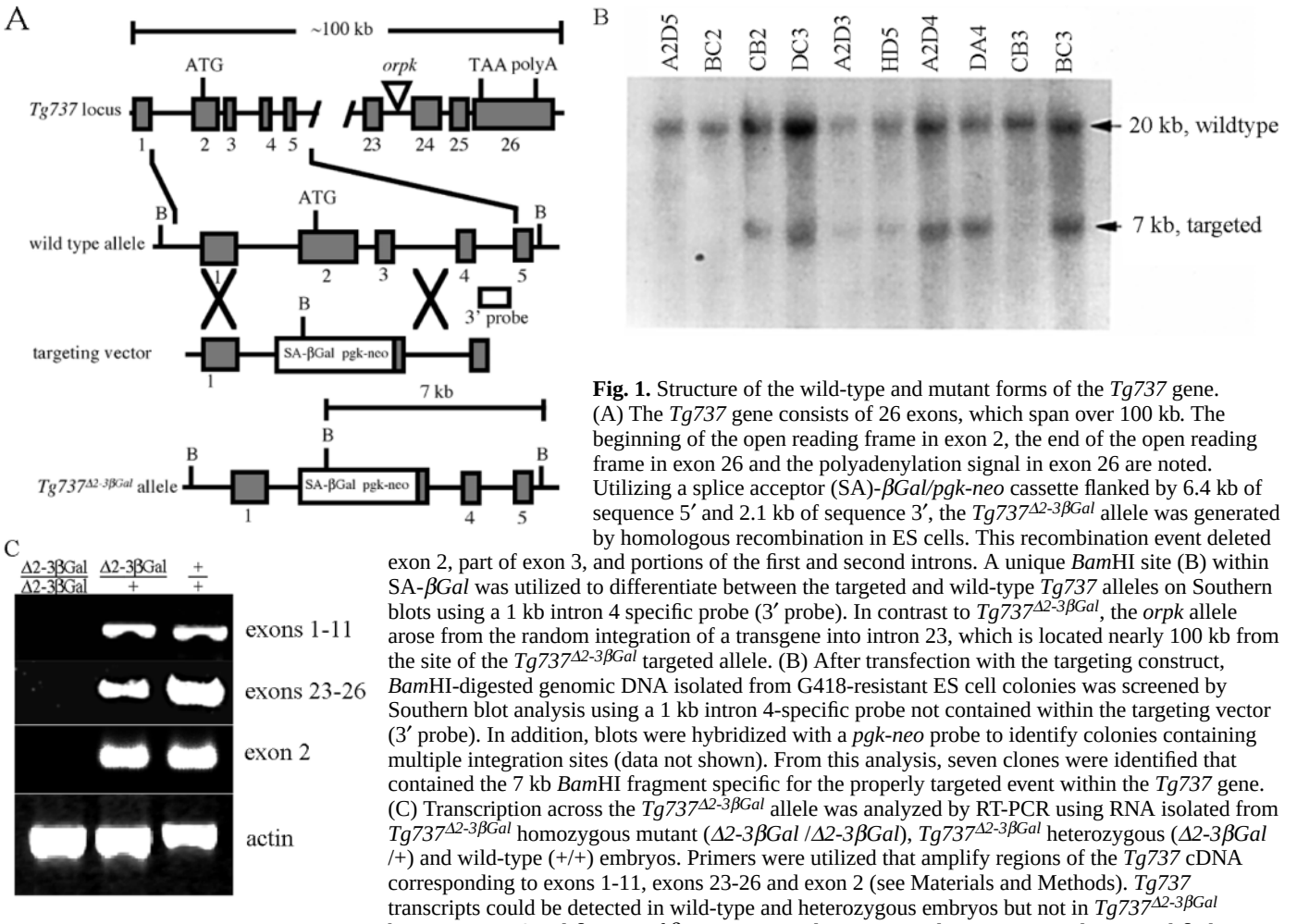

Fig. 1. Structure of the wild-type and mutant forms of the *Tg737* gene. (A) The *Tg737* gene consists of 26 exons, which span over 100 kb. The beginning of the open reading frame in exon 2, the end of the open reading frame in exon 26 and the polyadenylation signal in exon 26 are noted. Utilizing a splice acceptor (SA)-*βGal/pgk-neo* cassette flanked by 6.4 kb of sequence 5′ and 2.1 kb of sequence 3′, the $Tg737^{\Delta 2\text{-}3\beta Gal}$ allele was generated by homologous recombination in ES cells. This recombination event deleted exon 2, part of exon 3, and portions of the first and second introns. A unique *Bam*HI site (B) within SA-*βGal* was utilized to differentiate between the targeted and wild-type *Tg737* alleles on Southern blots using a 1 kb intron 4 specific probe (3′ probe). In contrast to $Tg737^{\Delta 2\text{-}3\beta Gal}$, the *orpk* allele arose from the random integration of a transgene into intron 23, which is located nearly 100 kb from the site of the $Tg737^{\Delta 2\text{-}3\beta Gal}$ targeted allele. (B) After transfection with the targeting construct, *Bam*HI-digested genomic DNA isolated from G418-resistant ES cell colonies was screened by Southern blot analysis using a 1 kb intron 4-specific probe not contained within the targeting vector (3′ probe). In addition, blots were hybridized with a *pgk-neo* probe to identify colonies containing multiple integration sites (data not shown). From this analysis, seven clones were identified that contained the 7 kb *Bam*HI fragment specific for the properly targeted event within the *Tg737* gene. (C) Transcription across the $Tg737^{\Delta 2\text{-}3\beta Gal}$ allele was analyzed by RT-PCR using RNA isolated from $Tg737^{\Delta 2\text{-}3\beta Gal}$ homozygous mutant (*Δ2-3βGal /Δ2-3βGal*), $Tg737^{\Delta 2\text{-}3\beta Gal}$ heterozygous (*Δ2-3βGal* /+) and wild-type (+/+) embryos. Primers were utilized that amplify regions of the *Tg737* cDNA corresponding to exons 1-11, exons 23-26 and exon 2 (see Materials and Methods). *Tg737* transcripts could be detected in wild-type and heterozygous embryos but not in $Tg737^{\Delta 2\text{-}3\beta Gal}$ homozygotes. Amplification of β-actin was used as an internal positive control. No amplified products were detected in the absence of reverse transcriptase (data not shown).

mutant embryos (Fig. 3A), we were interested in analyzing the temporal/spatial patterns of expression of the *Tg737* gene during early post-implantation development. Utilizing the *β-Gal* reporter function of the $Tg737^{\Delta 2\text{-}3\beta Gal}$ allele, we analyzed the expression of *Tg737* in heterozygous embryos during the egg cylinder, primitive streak and early somite stages of development (E6.5-E8.5). Although a low level of reporter expression was observed throughout E6.5-E8.5 embryos, high-level reporter expression was evident only in the ventral layer of the node of primitive streak-stage embryos (Fig. 3B,C). We utilized mRNA whole-mount in situ hybridization with *Tg737* antisense RNA probes to verify that the *βGal* reporter on the $Tg737^{\Delta 2\text{-}3\beta Gal}$ allele faithfully recapitulates the endogenous pattern of *Tg737* expression (data not shown).

Defects in the node of $Tg737^{\Delta 2\text{-}3\beta Gal}$ mutant embryos

In addition to studying patterns of *Tg737* expression, we carefully analyzed embryos at early post-implantation stages of development for cellular and morphological defects, particularly at sites where the *Tg737* gene is normally expressed. Embryos at E9.5 were slightly runted and exhibited neural tube defects (Fig. 3A). At earlier gestational ages (E6.5-E8.5), mutants were morphologically indistinguishable from their heterozygous and wild-type littermates when inspected by light microscopy.

To improve our sensitivity for detecting cellular defects in the mutant embryos, we imaged E7.5 embryos, which express the *Tg737* gene at relatively high levels in the node, with scanning electron microscopy (SEM). SEM analysis of whole embryos revealed that the individual cells on the surface of the node are different in embryos that are heterozygous from those that are homozygous for the $Tg737^{\Delta 2\text{-}3\beta Gal}$ mutation. In wild-type embryos, the ventral node cells located between the primitive streak and prechordal plate form a tight cluster of small, polarized epithelial cells, which express a monocilium on their apical cell surface (Sulik et al., 1994). Analysis of homozygous mutant embryos revealed that these cilia are absent from the surface of ventral node cells (Fig. 4). Therefore, utilizing SEM we were able to detect a clear cellular defect associated with the node of the mutant embryos.

$Tg737^{\Delta 2\text{-}3\beta Gal}$ is required for left-right axis determination

Midgestational lethality and node abnormalities similar to those observed with our $Tg737^{\Delta 2\text{-}3\beta Gal}$ mutants are also associated with the inactivation of the microtubule-dependent

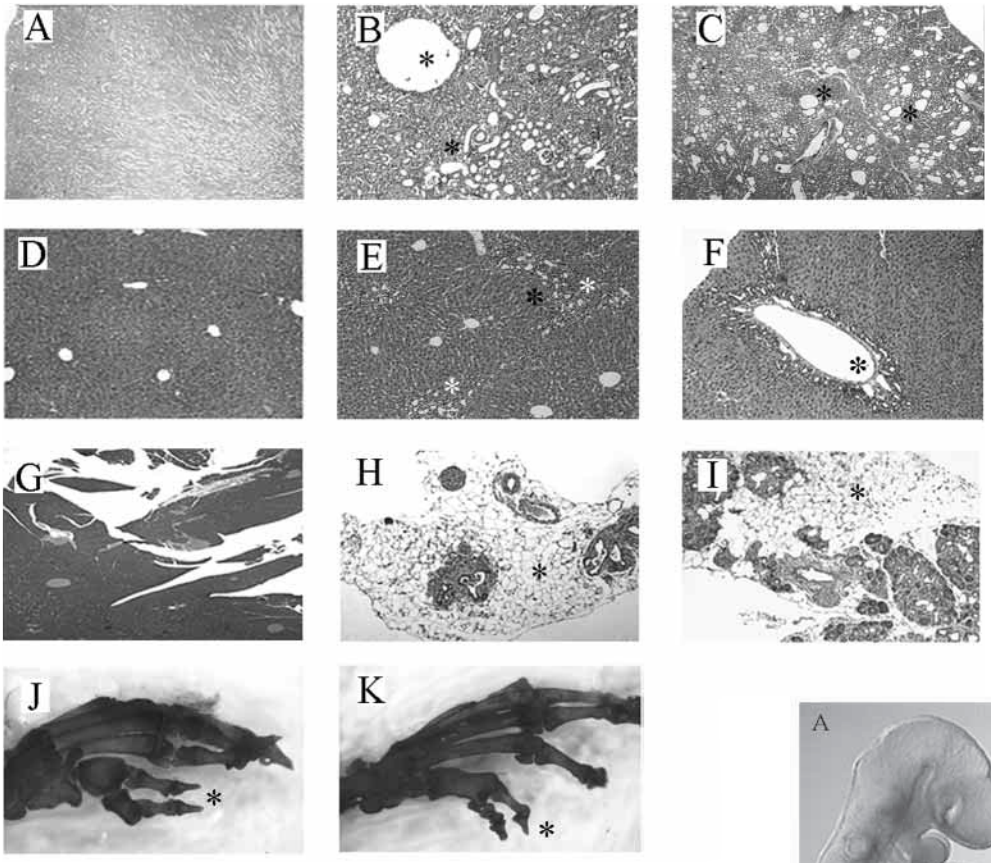

Fig. 2. The targeted mutation *Tg737*$^{\Delta 2\text{-}3\beta Gal}$ and the *orpk* insertional mutation are allelic. Comparison of *Tg737*$^{\Delta 2\text{-}3\beta Gal}$*/orpk* compound heterozygous and *orpk* homozygous mutant phenotypes on a mixed FVB/N-129/Sv genetic background. (A,D,G) Wild-type kidney, liver and pancreas sections, for comparison. Compound *Tg737*$^{\Delta 2\text{-}3\beta Gal}$*/orpk* heterozygotes (B,E,H,J) recapitulate the entire phenotype of *orpk* homozygous mutants (C,F,I,K). These lesions include (B,C) proximal tubule dilations and collecting duct cysts in the kidney (asterisks placed near cystic lesions in B,C), (E,F) biliary and bile ductular hyperplasia in the liver (noted by asterisks), (H,I) acinar cell atrophy and ductular hyperplasia in the pancreas (asterisks mark areas of cellular atrophy), and (J,K) preaxial polydactyly on both the fore- and hind-limbs (asterisks; hind-limb shown).

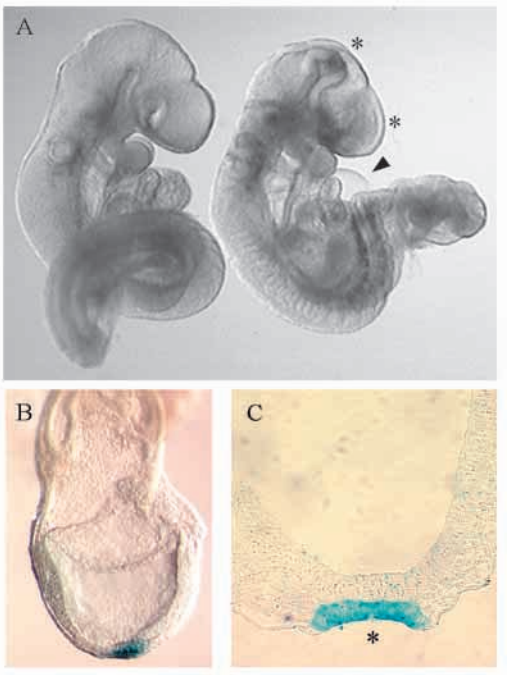

Fig. 3. (A) Mid-gestational lethal phenotype of *Tg737*$^{\Delta 2\text{-}3\beta Gal}$ homozygotes. *Tg737*$^{\Delta 2\text{-}3\beta Gal}$ homozygotes (right embryo) exhibit anterior defects (see asterisks), and mild undulations and kinks of the neural tube compared to heterozygous littermates (left embryo). Also apparent in this homozygous embryo is an expanded pericardial sac (arrowhead). Heterozygotes are phenotypically indistinguishable from wild-type littermates at all gestational ages analyzed and as adults. (B,C) Expression of the *Tg737*$^{\Delta 2\text{-}3\beta Gal}$ reporter allele in ventral node cells. Utilizing the *β-gal* reporter gene, expression of *Tg737* was detected in the ventral layer of the node. (B) Primitive streak-staged (E7.5) heterozygous embryos were stained in X-gal assays to reveal β-gal activity at the distal tip of the embryo in the node. The anterior aspect is left, ventral is down. (C) Cross section through E7.5 heterozygous *Tg737*$^{\Delta 2\text{-}3\beta Gal}$ embryos reveals high level *β-gal* reporter gene expression only in ventral node cells (asterisk).

motor protein *KIF3B* (Nonaka et al., 1998). The fact that the *KIF3B* mutants exhibit left-right asymmetry defects led us to test whether the *Tg737*$^{\Delta 2\text{-}3\beta Gal}$ also exhibit left-right polarity abnormalities. Gross morphological comparisons between E9.5 *Tg737*$^{\Delta 2\text{-}3\beta Gal}$ homozygous mutants revealed that the direction of heart looping was frequently reversed (Fig. 5G,H). Analysis of 25 E9.5 homozygous mutants revealed a random distribution of normal versus reversed heart looping, indicating that the *Tg737* gene is required for left-right axis determination: for wild-type and heterozygous embryos, 36/36 showed situs solitus (100%) and 0/36 situs inversus; for homozygous mutants, 12/25 showed situs solitus (48%) and 13/25 situs inversus (52%).

To determine where *Tg737* functions in the left-right pathway, whole-mount RNA in situ hybridization was utilized to analyze the expression patterns of known left-right marker genes in *Tg737*$^{\Delta 2\text{-}3\beta Gal}$ homozygous mutants. *Lefty-2* and *nodal* are members of the TGF-β superfamily of secreted polypeptide factors that are normally asymmetrically expressed along the L-R axis and function early in the left-right pathway (Meno et al., 1998; Collignon et al., 1996; Lowe et al., 1996). We evaluated the expression of Lefty-2 and nodal in both wild-type and mutant embryos at E8.0. Normally *lefty-2* is expressed in the left lateral plate mesoderm (Fig. 5A left embryo, B), and *nodal* expression overlaps with *lefty-2* in the left lateral plate mesoderm and is also expressed in an asymmetric pattern around the murine node (Fig. 5D left embryo, E,I). In *Tg737*$^{\Delta 2\text{-}3\beta Gal}$ homozygous mutants, we observed bilateral expression of the *lefty-2* and *nodal* genes in

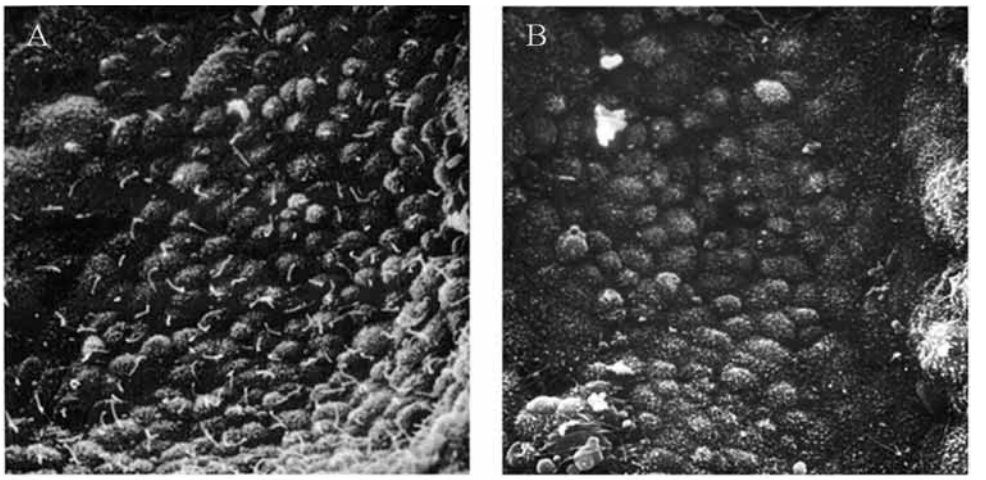

Fig. 4. Ventral node cells of *Tg737$^{\Delta 2\text{-}3\beta Gal}$* homozygotes lack cilia on their apical surface. SEM analysis of heterozygous (A) and homozygous *Tg737$^{\Delta 2\text{-}3\beta Gal}$* (B) embryos revealed defects in the ventral node of homozygous mutant embryos. Ventral node cells normally express a single cilium on their ventral surface (A), which is not apparent on the ventral node cells of *Tg737$^{\Delta 2\text{-}3\beta Gal}$* homozygotes. Scanning electron micrographs were obtained at 1500× magnification. The anterior aspect of the node is at the top of these photomicrographs.

both the left and right lateral plate mesoderm (Fig. 5A,D right embryos, C,F). Additionally, nodal was expressed in a bilateral pattern around the node in the mutant embryos (Fig. 5D right embryo, J).

Tg737$^{\Delta 2\text{-}3\beta Gal}$ homozygotes exhibit neural tube defects in addition to left-right axis defects. To better understand the molecular nature of the neural tube defects we analyzed the expression of *Shh* and *Hnf3β* by whole-mount mRNA in situ hybridization. We focused our analysis on E8.0 embryos in order to correlate early neural tube development with the transient expression of the left-right marker genes *lefty-2* and *nodal*. Wild-type E8.0 embryos normally expressed *Shh* in the presumptive floorplate and headfolds (Fig. 6A, left embryo). In E8.0 *Tg737$^{\Delta 2\text{-}3\beta Gal}$* homozygotes *Shh* expression remains confined to the presumptive floorplate and headfolds, although a slightly reduced level of *Shh* signal is reproducibly observed (Fig. 6A, right embryo). *Hnf3β* is normally expressed in the node, presumptive floorplate and headfolds of E8.0 wild-type embryos (Fig. 6B, left embryo). In *Tg737$^{\Delta 2\text{-}3\beta Gal}$* homozygotes *Hnf3β* expression is dramatically altered. Expression in the node is maintained, expression in the developing headfolds is qualitatively reduced and the presumptive floorplate does not appear to express significant levels of *Hnf3β* mRNA (Fig. 6B, right embryo). *Brachyury* (*T*) is expressed along the midline of primitive streak-stage embryos and it is required for mesoderm and notochord formation (Wilkinson et al., 1990). To rule out any major defects during mesoderm or notochord formation, we analyzed *T* expression in E8.0 *Tg737$^{\Delta 2\text{-}3\beta Gal}$* homozygotes. No abnormalities in *T* expression were found, indicating that *Tg737* is not required for *T* expression and, that mesoderm and notochord form normally in *Tg737$^{\Delta 2\text{-}3\beta Gal}$* homozygous mutants (Fig. 6C,D).

DISCUSSION

Tg737$^{\Delta 2\text{-}3\beta Gal}$ and *orpk* are allelic

Previously we described the o*rpk* insertional mutation, which represents a useful mouse model for ARPKD (Moyer et al., 1994; Yoder et al., 1995). Characterization of the *orpk* mutant locus led to the identification of the *Tg737* gene, which is directly associated with the phenotype in this model (Moyer et al., 1994). Here we describe another allele of the *Tg737* gene, *Tg737$^{\Delta 2\text{-}3\beta Gal}$*, which replaces the first and part of the second coding exons with a combination splice acceptor-*βGal/pgk-neo* expression cassette (Fig. 1A). This mutation disrupts transcription across the *Tg737* locus (Fig. 1C) and places the *β-Gal* reporter gene under the control of endogenous *Tg737* regulatory elements. This new mutation completely inactivates the activity of the gene. The fact that animals homozygous for the *Tg737$^{\Delta 2\text{-}3\beta Gal}$* allele exhibit left-right symmetry defects and arrest in development at about E10.5 defines a new and critical function for the *Tg737* gene during embryogenesis.

Our finding that knocking out the *Tg737* gene causes a more severe phenotype than the *orpk* allele suggests that the original insertional mutation is a hypomorphic allele of *Tg737*. This is compatible with our previous finding that, although the primary transcript of 3.2 kb is not expressed from the *orpk* locus, other low-abundance higher-molecular mass transcripts can still be detected on a northern blot using RNA from the *orpk* mutants (Moyer et al., 1994). These residual transcripts may represent low abundance and normal alternatively spliced forms of mRNA that are not affected by the inserted transgene, or they may represent aberrant transcripts that arise from the unique configuration of the DNA at the mutant locus. These residual transcripts must still produce a functional gene product that rescues the embryos through development, since we have not detected any degree of embryonic lethality associated with the *orpk* allele. Whether any gene product arising from the mutant locus is normal or abnormal is not clear. Further analysis of the transcripts arising from the *orpk* allele will help to resolve this issue.

Also, in the process of characterizing the new *Tg737$^{\Delta 2\text{-}3\beta Gal}$* targeted allele we resolved an issue that arose in our earlier gene rescue experiments. Expression of a full-length *Tg737* cDNA as a transgene rescued the kidney, but not the liver and pancreatic defects, in *orpk* homozygotes (Yoder et al., 1996). This raised the possibility that a disruption of a second closely linked gene could be contributing to the pleiotrophy associated with the *orpk* allele, particularly in the liver and pancreas (Yoder et al., 1997). Here we demonstrate that this is unlikely to be the case. Although *Tg737$^{\Delta 2\text{-}3\beta Gal}$* homozygotes and *orpk* homozygotes exhibit dramatically different phenotypes, it is noteworthy that compound heterozygotes (*Δ2-3βGal*/*orpk*) are phenotypically identical to *orpk* homozygotes (Fig. 2). This

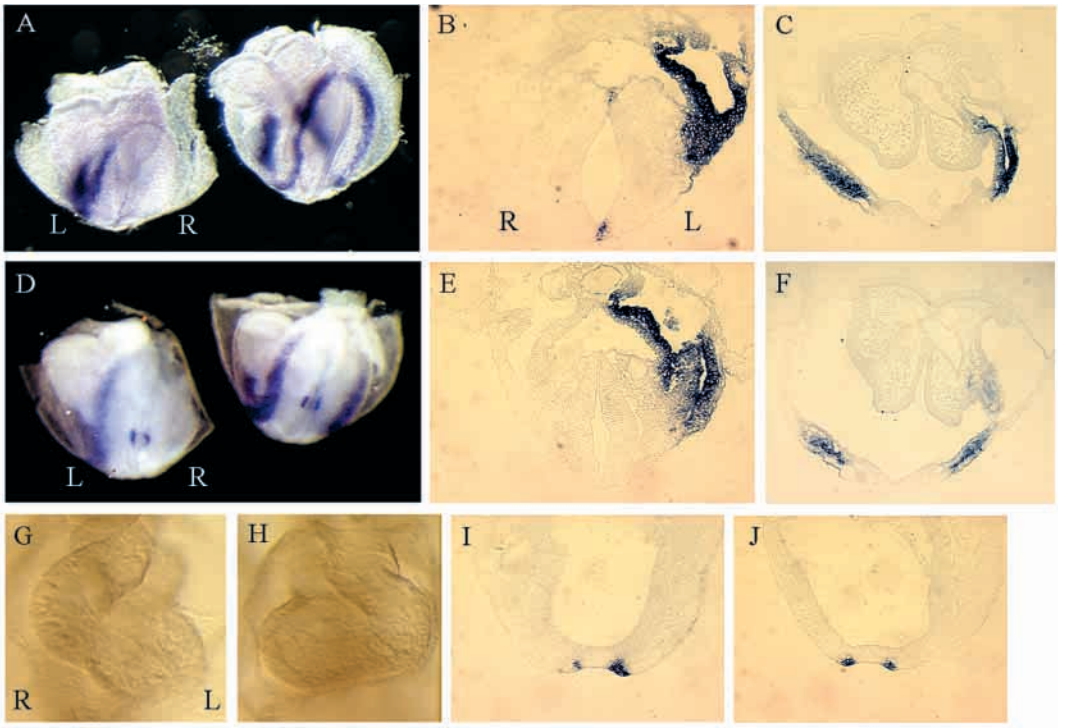

Fig. 5. Randomization of left-right asymmetry in *Tg737*$^{\Delta 2\text{-}3\beta Gal}$ homozygotes. mRNA in situ analysis in E8.0 embryos reveals early defects in the molecular pathway of left-right axis determination. (A) Posterior view of *lefty-2* expression in heterozygous and homozygous *Tg737*$^{\Delta 2\text{-}3\beta Gal}$ embryos reveals normal *lefty-2* expression in heterozygotes (left embryo) and bilateral expression of *lefty-2* in homozygous mutants (right embryo). L and R indicate the left and right sides of the embryos, respectively. Cross sections through whole-mount embryos reveals *lefty-2* expression in the left lateral plate mesoderm of heterozygotes and *lefty-2* expression in both the left and right lateral plate mesoderm in homozygous mutants (B and C, respectively). (D) Posterior view of *nodal* expression in heterozygous and homozygous *Tg737*$^{\Delta 2\text{-}3\beta Gal}$ embryos reveals normal expression of *nodal* in heterozygotes (left embryo) and bilateral expression of *nodal* in both the lateral plate mesoderm and around the node in homozygous mutants (right embryo). Cross sections through whole-mount embryos reveal *nodal* expression in the left lateral plate mesoderm of heterozygotes and the left and right lateral plate mesoderm of homozygous mutants (E and F, respectively). More posterior sections through the node reveal asymmetrical *nodal* expression in heterozygotes and symmetrical expression of *nodal* in homozygous mutants (I and J, respectively). (G,H) Comparison of E9.5 *Tg737*$^{\Delta 2\text{-}3\beta Gal}$ homozygous mutants reveals frequent reversal of heart left-right determination. One homozygous mutant heart exhibits situs solitus (G) whereas the other exhibits situs inversus (H).

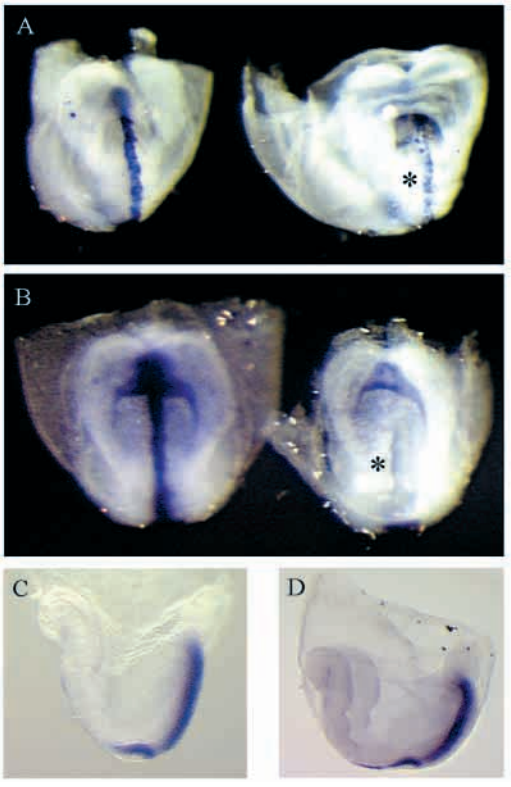

non-complementation strongly suggests that *Tg737* is the one and only gene associated with the mutant phenotype in the *orpk* mutant animals.

The role of *Tg737* in left-right asymmetry

Analysis of the *Tg737*$^{\Delta 2\text{-}3\beta Gal}$ homozygotes revealed that the ventral node is the site where we detect the first apparent structural abnormalities in the embryo. The murine node is a bilayer composed dorsally of ectoderm and ventrally of small, polarized cells, which express a single cilium on their apical

Fig. 6. Evidence for a midline defect in *Tg737*$^{\Delta 2\text{-}3\beta Gal}$ homozygotes. (A,B) Whole-mount mRNA in situ analysis in E8.0 embryos reveals defects in midline development. (A) Anterior view of *Shh* expression in heterozygous and homozygous *Tg737*$^{\Delta 2\text{-}3\beta Gal}$ embryos reveals normal *Shh* expression in heterozygotes (A, left embryo) and reduced *Shh* expression in homozygous mutants (A, right embryo; asterisk). (B) Anterior view of *Hnf3β* expression in heterozygous and homozygous mutants reveals normal *Hnf3β* expression in heterozygotes (B, left embryo) and normal expression in the node of homozygous mutants (B, right embryo). Homozygous mutants do not exhibit staining for *Hnf3β* mRNA in the midline between the node and headfolds and they exhibit reduced staining in the headfolds (B, right embryo; asterisk). (C,D) *Brachyury* expression was utilized as a control for mesoderm development. In both heterozygous and homozygous *Tg737*$^{\Delta 2\text{-}3\beta Gal}$ embryos (C and D, respectively), staining is apparent in the primitive streak and node, with faint staining along the notochord.

surface (Sulik et al., 1994; Bellomo et al., 1996). Although structurally different, the murine node is functionally analogous to Hensen's node in chick, Spemann's organizer in *Xenopus* and the embryonic shield in zebrafish. These structures possess organizer activity, which is defined by their ability to induce a second embryonic axis after heterotropic grafting (Beddington, 1994; Waddington, 1932; Spemann and Mangold, 1924; Shih and Fraser, 1996).

Evidence from several reports suggests that node function is required for left-right axis determination. In vitro culture experiments helped to define the window during which left-right axis determination occurs. Specification of left-right asymmetry is not sensitive to in vitro culture after early headfold stages (E8.0; Fujinaga and Baden, 1991; McCarthy and Brown, 1998), which indicates that left-right axis determination occurs at or before E8.0. Node ablation experiments where the node is physically removed from the primitive streak-staged embryo increase left-right defects during in vitro culture, implicating node function or node-derived tissues in left-right axis determination (Davidson et al., 1999).

Additional data suggests that ventral node cells may function early in the left-right pathway. Nonaka et al. (1998) discovered that a targeted disruption of *KIF3B* causes a loss of cilia on ventral node cells and left-right defects in the embryo. They hypothesized that synchronized movement of ventral node cilia creates a 'nodal flow' across the node surface that causes a relative difference in the concentration of factors over the surface of the node. These relative differences in factor concentration are thought to cause differential signaling in the left and right sides of the node, and this in turn could be the basis for establishing the left-right axis in the embryo. Mutations that eliminate the cilia from the surface of ventral node cells would block nodal flow and block the development of any differential concentrations of signaling factors on the left and right sides of the node. This is potentially one possible explanation for the left-right polarity defects exhibited by both the *KIF3B* and *Tg737* mutant embryos.

Alternatively, the fact that $Tg737^{\Delta 2\text{-}3\beta Gal}$ and *KIF3B* mutants also exhibit neural tube defects (NTDs) may indicate that these mutants possess a midline defect, which causes both the left-right alterations and NTDs. Defects in the development of the notochord and/or floorplate may cause NTDs and affect left-right development by disrupting the midline barrier (Meno et al., 1998).

In $Tg737^{\Delta 2\text{-}3\beta Gal}$ homozygous mutants we have evidence for a midline defect. In E8.0 homozygotes, *Shh* mRNA is reduced and *Hnf3β* mRNA is dramatically absent in the developing floorplate and notochord (Fig. 6). Altered expression of these genes indicates that the floorplate and/or notochord in $Tg737^{\Delta 2\text{-}3\beta Gal}$ homozygous mutants may not function properly. Therefore, independent of cilia defects in the node (Fig. 4), left-right development may be compromised by an abnormal midline in $Tg737^{\Delta 2\text{-}3\beta Gal}$ homozygous mutants.

The loss of ventral node cilia and an abnormal midline in $Tg737^{\Delta 2\text{-}3\beta Gal}$ homozygous mutants may be developmentally linked. As the primitive streak-staged embryo grows and elongates, ventral node cells migrate out of the node and contribute to the midline. Although the ventral node and notochord are contiguous in primitive streak-staged embryos, theoretically there must be a boundary where the migrating cells from the ventral node become committed to midline structures, such as the notochord and/or floorplate. In E8.0 wild-type and $Tg737^{\Delta 2\text{-}3\beta Gal}$ heterozygous embryos, *Hnf3β* is expressed in both node and notochord and does not reveal any boundary between these structures. In E8.0 $Tg737^{\Delta 2\text{-}3\beta Gal}$ homozygous mutant embryos, node cells express *Hnf3β*; however, notochord cells fail to express *Hnf3β* (Fig. 6B). This dramatic loss of *Hnf3β* expression at the anterior edge of the node in E8.0 $Tg737^{\Delta 2\text{-}3\beta Gal}$ homozygous mutant embryos appears to delineate the boundary between the ventral node and the developing notochord and floorplate. Primitive streak-staged $Tg737^{\Delta 2\text{-}3\beta Gal}$ homozygous mutants do not appear to be able to maintain *Hnf3β* expression during the transition from node to notochord/floorplate. This loss of *Hnf3β* expression in the developing midline indicates that these mutants have a midline defect, which appears to be derived from abnormal or incomplete differentiation of the ventral node epithelium.

The polarity connection

We have now analyzed the kidney phenotype of the *orpk* allele and the node and early embryonic defects associated with the $Tg737^{\Delta 2\text{-}3\beta Gal}$ targeted mutation. In both mutations there are changes in polarized epithelial cells that appear to underlie the mutant phenotype. In $Tg737^{\Delta 2\text{-}3\beta Gal}$ homozygotes, the polarized epithelial cells of the ventral node are affected. In the *orpk* homozygotes, cystic lesions develop as a consequence of the ectopic expansion of a population of polarized epithelial cells of the collecting duct, called principal cells (Sweeney and Avner, 1998). Both cell types have a central cilium. Additionally, we have recently determined that the cellular defect in the collecting duct involves abnormal polarity of the EGF receptor (EGFR). Normally the EGFR is localized strictly on the basolateral surface of epithelial cells in collecting duct, but it is mislocalized to the apical surface of epithelial cells (principal cells) which line the lumen of collecting duct cysts (Richards et al., 1998).

Although it is presently unclear whether there are also polarity defects associated with the positioning of molecules like the EGFR on the node, it is noteworthy that the node defects predispose the embryos to develop left-right polarity defects during early embryogenesis. Therefore, polarity defects at both the cellular and multicellular level are associated with mutations in the *Tg737* gene. Our best estimation is that the *Tg737* gene plays a critical role in the development and maintenance of polarized epithelium in the embryo and the kidney, and changes in the epithelium in mutant animals are responsible for the phenotypes that we observe.

Polaris, the protein product of the *Tg737* gene

The sequence of the *Tg737* cDNA clone predicts a novel 824 amino acid protein. This protein contains ten copies of the tetratricopeptide repeat, a motif that was originally defined based on its conservation in several cell-cycle control genes (Goebl and Yanagida, 1991; Lamb et al., 1994). The presence of TPRs in many diverse proteins appears to point toward a protein structure that may mediate diverse protein-protein interactions (Groves and Barford, 1999). We originally named the *Tg737* gene because it arose in the 737th transgenic line that was screened for insertional mutations at the Oak Ridge National Laboratory. Here we propose to name the *Tg737* gene product Polaris, which refers to both the polarity defects in the

positioning of the EGFR and to the left-right polarity defects in the early embryo. We believe that this name for the gene product better reflects our current understanding of the underlying functions of the *Tg737* gene at both the cellular and multi-cellular levels.

We thank Carmen Foster, Eugene Barker and Nicole Brown for their expert technical assistance. We would also like to thank Dr Kumar Alagramam, Crystal Rohrbaugh, Dr Terry Magnuson, and Dr Ellis Avner for critical comments on this manuscript. This research was supported in part by a Eugene P. Wigner Distinguished Postdoctoral Fellowship (W.G.R.), sponsored by the Oak Ridge National Laboratory, and by an Alexander Hollaender Distinguished Postdoctoral Fellowship (B.K.Y.), sponsored by the US Department of Energy. In addition, this work was funded by National Institutes of Health Grant DK51068 (R.P.W.).

REFERENCES

Beddington, R. S. (1994). Induction of a second neural axis by the mouse node. *Development* **120**, 613-620.

Bellomo, D., Lander, A., Harragan, I. and Brown, N. A. (1996). Cell proliferation in mammalian gastrulation: the ventral node and notochord are relatively quiescent. *Dev. Dyn.* **205**, 471-485.

Casey, B. (1998). Two rights make a wrong: human left-right malformations. *Hum. Mol. Genet*. **7**, 1565-1571.

Collignon, J., Varlet, I. and Robertson, E. J. (1996). Relationship between asymmetric *nodal* expression and the direction of embryonic turning. *Nature* **381**, 155-158.

Davidson, B. P., Kinder, S. J., Steiner, K., Schoenwolf, G. C. and Tam, P. P. L. (1999). Impact of node ablation on the morphogenesis of the body axis and the lateral asymmetry of the mouse embryo during early organogenesis. *Dev. Biol.* **211**, 11-26.

Fujinaga, M. and Baden J. M. (1991). Critical period of rat development when sideness of asymmetric body structure is determined. *Teratology* **44**, 453-462.

Goebl, M. and Yanagida, M. (1991). The TPR snap helix: a novel protein repeat motif from mitosis to transcription. *Trends Biochem. Sci*. **16**, 173-177.

Groves, M. R. and Barford, D. (1999). Topological characteristics of helical repeat proteins. *Curr. Opin. Struct. Biol.* **9**, 383-389.

Henrique, D., Adam, J., Myat, A., Chitnis, A., Lewis, J. and Ish-Horowicz, D. (1995). Expression of a Delta homologue in prospective neurons in the chick. *Nature* **375**, 787-790.

Hogan B., Beddington R., Costantini F. and Lacy E. (1994). *Manipulating the Mouse Embryo*. Cold Spring Harbor Press, Cold Spring Harbor, New York.

Lamb, J. R., Michaud, W. A., Sikorski, R. A. and Hieter, P. A (1994). Cdc16p, Cdc23p and Cdc27p form a complex essential for mitosis. *EMBO J.* **13**, 4321-4328.

Lowe, L. A., Supp, D. M., Sampath, K., Yokoyama, T., Wright, C. V. E., Potter, S. S., Overbeek, P. and Kuehn, M. R. (1996). Conserved left-right asymmetry of nodal expression and alterations in murine *situs inversus*. *Nature* **381**, 158-161.

McCarthy, A. and Brown, N. A. (1998). Specification of left-right asymmetry in mammals: embryo culture studies of stage of determination and relationships with morphogenesis and growth. *Reprod. Toxicol*. **12**, 177-184.

Meno, C., Shimono, A., Saijoh, Y., Oishi, S., Mochida, S., Noji S., Kondoh, H. and Hamada, H. (1998). *lefty-1* is required for left-right determination as a regulator of *lefty-2* and *nodal*. *Cell* **94**, 287-298.

Mochizuki, T. et al. (1998). Cloning of *inv*, a gene that controls left/right asymmetry and kidney development. *Nature* **395**, 177-181.

Morgan, D. et al. (1998). Inversin, a novel gene in the vertebrate left-right axis pathway, is partially deleted in the *inv* mouse. *Nature Genetics* **20**, 149-156.

Moyer, J. H., Lee-Tischler, M. J., Kwon, H., Schrick, J. J., Avner, E. D., Sweeney, W. E., Godfrey, V. L., Cacheiro, N. L. A., Wilkinson, J. E. and Woychik, R. P. (1994). Candidate gene associated with a mutation causing recessive polycystic kidney disease in mice. *Science* **264**, 1329-1333.

Murcia, N. S., Woychik, R. P. and Avner, E. D. (1998). The molecular biology of polycystic kidney disease. *Ped. Nephrol*. **12**, 721-726.

Murcia, N. S., Sweeney, W. E. and Avner, E. D. (1999). New insights into the molecular pathophysiology of polycystic kidney disease. *Kidney Int.* **55**, 1187-1197.

Nonaka, S., Tanaka, Y., Okada, Y., Takeda, S., Harada, A., Kanai, Y., Kido, M. and Hirokawa, N. (1998). Randomization of left-right asymmetry due to loss of nodal cilia generating leftward flow of extraembryonic fluid in mice lacking KIF3B motor protein. *Cell* **95**, 829-837.

Richards, W. G., Sweeney, W. E., Yoder, B. K., Wilkinson, J. E., Woychik, R. P. and Avner, E. D. (1998). Epidermal growth factor receptor activity mediates renal cyst formation in polycystic kidney disease. *J. Clin. Invest.* **101**, 935-939.

Ryan, A. K. et al. (1998). Pitx2 determines left-right asymmetry of internal organs in vertebrates. *Nature* **394**, 545-551.

Sambrook J., Fritsch E. F. and Maniatis T. (1989). *Molecular Cloning*. Cold Spring Harbor Press, Cold Spring Harbor, New York.

Shih, J. and Fraser, S. E. (1996). Characterizing the zebrafish organizer: Microsurgical analysis at the early-shield stage. *Development* **122**, 1313-1322.

Spemann, H. and Mangold, H. (1924). Uber induction von embryonanlagen durch implantation artfremder organis atoren. *Roux's Arch. Dev. Biol*. **100**, 599-638.

Sulik, K., Dehart, D. B., Inagaki, T., Carson, J. L., Vrablic, T., Gesteland, K. and Schoenwolf, G. C. (1994). Morphogenesis of the murine node and notochordal plate. *Dev. Dyn.* **201**, 260-278.

Supp, D. M., Witte, D. P., Potter, S. S. and Brueckner, M. (1997). Mutation of an axonemal dynein affects left-right asymmetry in *inversus viscerum* mice. *Nature* **389**, 963-966.

Sweeney, W. E. and Avner, E. D. (1998). Functional activity of epidermal growth factor receptors in autosomal recessive polycystic kidney disease. *Am. J. Physiol.* **275**, F387-394.

Waddington, C. H. (1932). Experiments on the development of the chick and the duck embryo cultivated in vitro. *Proc. Trans. R. Soc. Lond.* **211**, 179-230.

Wilkinson, D. G., Bhatt, S. and Herrmann, B. G. (1990). Expression pattern of the mouse T gene and its role in mesoderm formation. *Nature* **343**, 657-659.

Yoder, B. K., Richards, W. G., Sweeney, W. E., Wilkinson, J. E., Avner, E. D. and Woychik, R. P. (1995). Insertional mutagenesis and molecular analysis of a new gene associated with polycystic kidney disease. *Proc. Assoc. Am. Phys.* **103**, 314-323.

Yoder, B. K., Richards, W. G., Sommardahl, C., Sweeney, W. E., Michaud, E. J., Wilkinson, J. E., Avner, E. D. and Woychik, R. P. (1996). Functional correction of renal defects in a mouse model for ARPKD through expression of the cloned wild-type Tg737 cDNA. *Kidney Int.* **50**, 1240-1248.

Yoder, B. K., Richards, W. G., Sommardahl, C., Sweeney, W. E., Michaud, E. J., Wilkinson, J. E., Avner, E. D and Woychik, R. P. (1997). Differential rescue of the renal and hepatic disease in an autosomal recessive polycystic disease mouse mutant. A new model to study the liver lesion. *Am. J. Pathol.* **150**, 2231-2241.